

## Shape-selection through epitaxy of supported platinum nanocrystals

### Electronic Supplementary Material

Laurent Peres,<sup>a</sup> Deliang Yi,<sup>a</sup> Susana Bustos-Rodriguez,<sup>a</sup> Cécile Marcelot,<sup>b</sup> Alexandre Pierrot,<sup>a</sup> Pier-Francesco Fazzini,<sup>a</sup> Ileana Florea,<sup>c</sup> Raul Arenal,<sup>d,e</sup> Lise-Marie Lacroix,<sup>a</sup> Bénédicte Warot-Fonrose,<sup>b</sup> Thomas Blon,<sup>a</sup> and Katerina Soulantica\*<sup>a</sup>

a. Laboratoire de Physique et Chimie des NanoObjets (LPCNO), Université de Toulouse, CNRS, INSA, UPS, 135 avenue de Rangueil, 31077 Toulouse, France.

b. Centre d'Elaboration de Matériaux et d'Etudes Structurales (CEMES-CNRS), 29 rue Jeanne Marvig, B.P. 94347, 31055 Toulouse, France.

c. Laboratoire de Physique des Interfaces et des Couches Minces (LPICM), Ecole Polytechnique/CNRS, Route de Saclay, 91128 Palaiseau Cedex, France.

d. Instituto de Nanociencia de Aragon (INA), Universidad de Zaragoza, Calle Mariano Esquillor, 50018 Zaragoza, Spain..

e. ARAID, 50018 Zaragoza, Spain.

### Materials and Methods

All syntheses were performed under inert conditions in order to avoid oxygen and water during the synthesis. After synthesis the nanoparticles were handled under ambient conditions. PtCl<sub>2</sub> 98% was obtained from Alfa Aesar, and kept in the glove-box freezer. Only freshly opened vials were used due to the instability of the precursor after vial opening. Octadecylamine (ODA - C<sub>18</sub>H<sub>39</sub>N, 98%) was purchased from Sigma-Aldrich. These products were introduced in a glovebox and used without any further purification. Toluene (99%) was purchased from VWR Prolabo, then purified on alumina desiccant and degassed through three freeze-pump-thaw cycles. Pentane (99%) and tetrahydrofuran (THF, 99%) were obtained from Sigma Aldrich.

Transmission electron microscopy (TEM) observations were carried using either a JEOL 1400 or a JEOL 2100F electron microscope operated at 200 keV.

The samples have been examined in high resolution electron microscopy (HREM) either on a JEOL 2100F or on a TECNAI F-20 microscope operating at 200 kV, equipped with a spherical aberration corrector to avoid the delocalization effect at interface and to achieve a 0.12 nm resolution.

The cross-sections of the concave nanocubes grown on Pt(111) at 25°C (Fig. 3) were prepared by Focused Ion Beam (FIB) to ensure a uniform thickness crossed by the electron beam. A 250 nm thick carbon layer was deposited to avoid damages during the thinning process. The lamella was then extracted and thinned down to about 100nm to get electron transparency with a final step at low energy to minimize irradiation damages and amorphization of the surfaces. The cross-section

specimen of the nano-objects grown at 100°C on Pt(111) (Fig. 4) has been prepared by using Ar ion thinning after a mechanical and dimple grind pre-thinning step.

Scanning electron microscopy (SEM) was carried out on a JEOL 6700F.

The electron tomography (ET) studies were performed in the Scanning Transmission Electron microscopy (STEM) mode of the FEI Titan Cube (80-300 kV) electron microscope using a 300kV accelerating voltage. The large inner radius of the High-Angle Annular Dark-Field (HAADF) detector used for the acquisition of the tilt series allowed us to consider, as a first approximation, that the intensity in the corresponding images is proportional to the mean atomic number of the specimen. The acquisition of tilt series was done automatically using the Inspect 3D tomography software, which controls the specimen tilt step by step, the defocusing, and the specimen drift. In the STEM mode, a projection image of the sample is obtained by scanning the sample with a focused probe in a raster pattern. The HAADF tilt series was acquired by tilting the specimen in the angular range of  $\pm 67^\circ$  using an increment of  $2^\circ$  in the equal mode, giving thus a total number of images equal to 67 images in the tilt series. The recorded images of the tilt series were spatially aligned using a rough alignment by cross correlating consecutive images, procedure implemented in the IMOD software (Mastronarde, D. N. J. Struct. Biol. 1997, 120, 343–352). For the volume calculation, we have used the algebraic reconstruction techniques (ART) implemented in the TomoJ plugin working in the ImageJ software (Gordon, R.; Bender, R.; Herman, G. T. J. Theor. Biol. 1970, 24, 471–481; Messaoudii, C.; Boudier, T.; Schancez Sorzano, C. O.; Marco, S. BMC Bioinf. 2007, 6, 288–292; <http://u759.curie.u-psud.fr/software/u759.html>). Finally, the visualization and the analysis of the final volumes were carried out using the displaying capabilities and the isosurface rendering method in the Slicer software. (<http://www.Slicer3D.org>)

The X-ray diffraction (XRD) measurements of Fig. S2 and S5 were performed on a  $\theta$ - $\theta$  PANalytical Empyrean diffractometer using a Co tube ( $\lambda_{\text{K}\alpha}^{\text{Co}} = 1.79031 \text{ \AA}$ ). The measurements of Fig. S8 were obtained on a  $\theta$ - $\theta$  4-circles PANalytical Empyrean diffractometer using a Co tube and Ge(220) monochromator to select Co  $\text{K}\alpha_1$  radiation ( $\lambda_{\text{K}\alpha_1}^{\text{Co}} = 1.78901 \text{ \AA}$ ). The ICDD database was used for the data interpretation.

#### Synthesis of nanoparticles in solution

For the preparation of concave cubes, the reactants,  $\text{PtCl}_2$  98% (16 mg), ODA (400 mg), and toluene (7 mL), were introduced in a Fischer Porter bottle in the glove box. After 10 min of homogenization of the mixture in an ultrasonic bath, the Fischer Porter bottle was charged with 3 bar of dihydrogen and then left at 20°C for 168 h (one week) under agitation. At the end of the reaction, the bottle was depressurized and the final suspension was diluted by adding 10 mL of toluene, redispersed with the aid of ultrasound short treatment (1 min), and 10 mL of ethanol were added. The mixture was centrifuged at 12 krpm for 10 minutes. After having removed the supernatant, 10 mL of toluene and 10 mL of ethanol were added. The operation was repeated three times. Finally, 10 mL of pentane were added and, after decantation and supernatant removal, the nanoparticles were dried under vacuum.

The same procedure was followed for all nanostructures obtained in solution. The only difference was the temperature and the reaction time, as indicated in the text.

## Growth of the nanoparticles on Pt(111)

The Pt(111) 20nm epitaxial films were deposited by sputtering at 500°C on  $\alpha\text{-Al}_2\text{O}_3$  (0001) substrates ( $1\times 1\text{ cm}^2$ ), according to (N. Liakakos et al, Nano Lett. 2014, 14, 3481–3486 and N. Liakakos, et al. ACS Nano 2015, 9, 9665–9677.

In the glove box, the reactants,  $\text{PtCl}_2$  98% (16 mg) ODA (400 mg), and toluene (7 mL), were introduced in a Fischer Porter bottle together with the Pt(111) support with the Pt(111) thin layer facing the bottom of the bottle. After homogenization in an ultrasonic bath, the Fischer Porter bottle was purged and charged with 3 bar of dihydrogen and left at 25°C for 168h without agitation. At the end of the reaction, the bottle was depressurized. The supernatant was removed and the substrate was washed three times with 10 mL of pentane, with 1min of ultrasonic bath between each steps.

The protocol for growing dendrites on Pt(111) was identical, with the difference that the support was added after homogenizing by ultrasounds to the  $\text{PtCl}_2$ -ODA toluene mixture and the reaction was kept at 100°C for 24h. Finally, the suspension was diluted by adding 10 mL of toluene and homogenized in the ultrasonic bath. The supernatant was removed and the substrate washed three times with 3 mL of toluene, three times with 3 mL of THF and three times with 3 mL of pentane, with 1min of ultrasonic bath between each step.

## Electron Tomography study of a concave cube

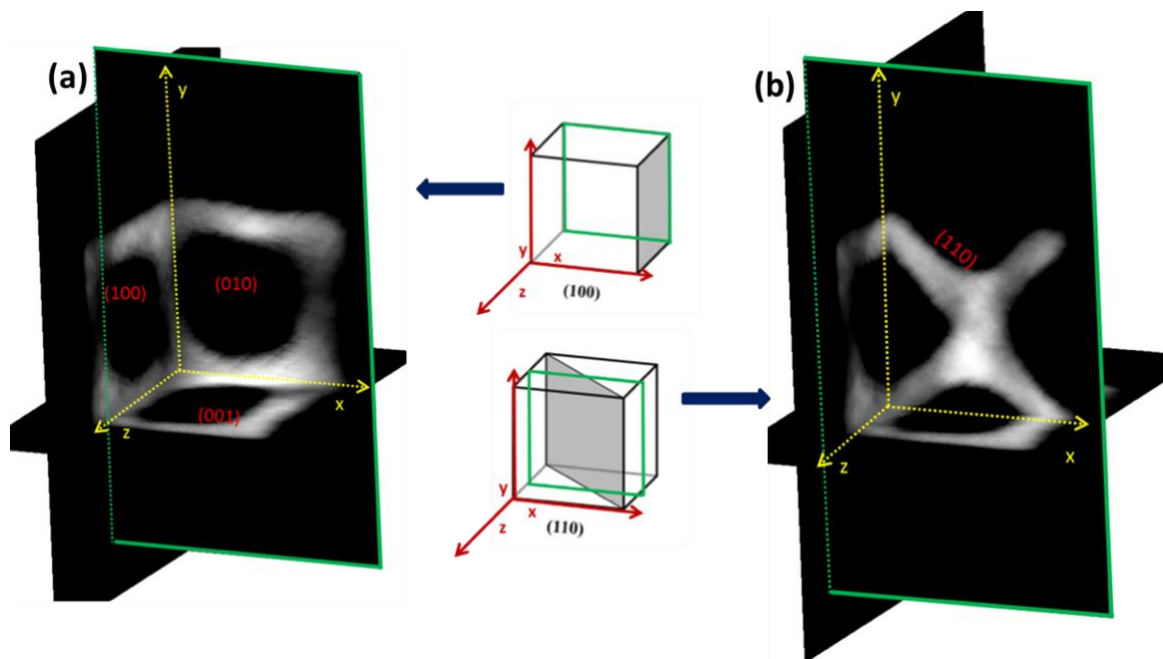


Fig. S1. (a) and (b) Orthogonal slices through the Pt nanocube reconstructed volume oriented in order to evidence its (100), (010) and (001) facets (a) and (110) inside the cube (b). In inset schematic representation of the procedure used to better indicate the position where the section along the Z-axis (green color) was taken through the reconstructed volume.

**XRD of the concave nanocubes**

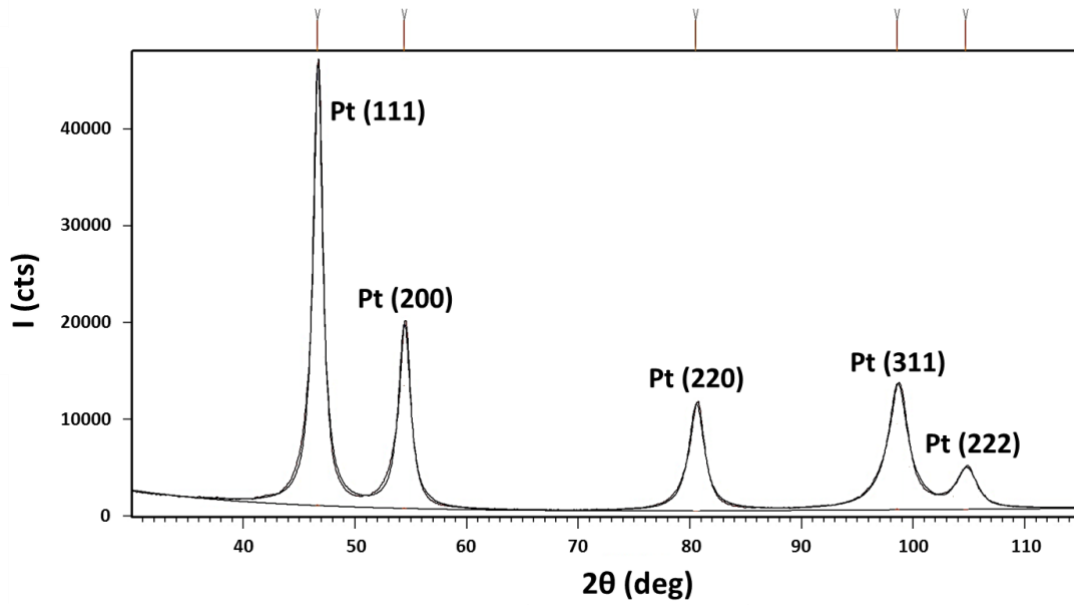


Fig. S2. XRD diffractogram of the concave cubes (Indexation of the peaks according to ICCD : 00-004-0802).

### Evolution in time of the concave nanocubes

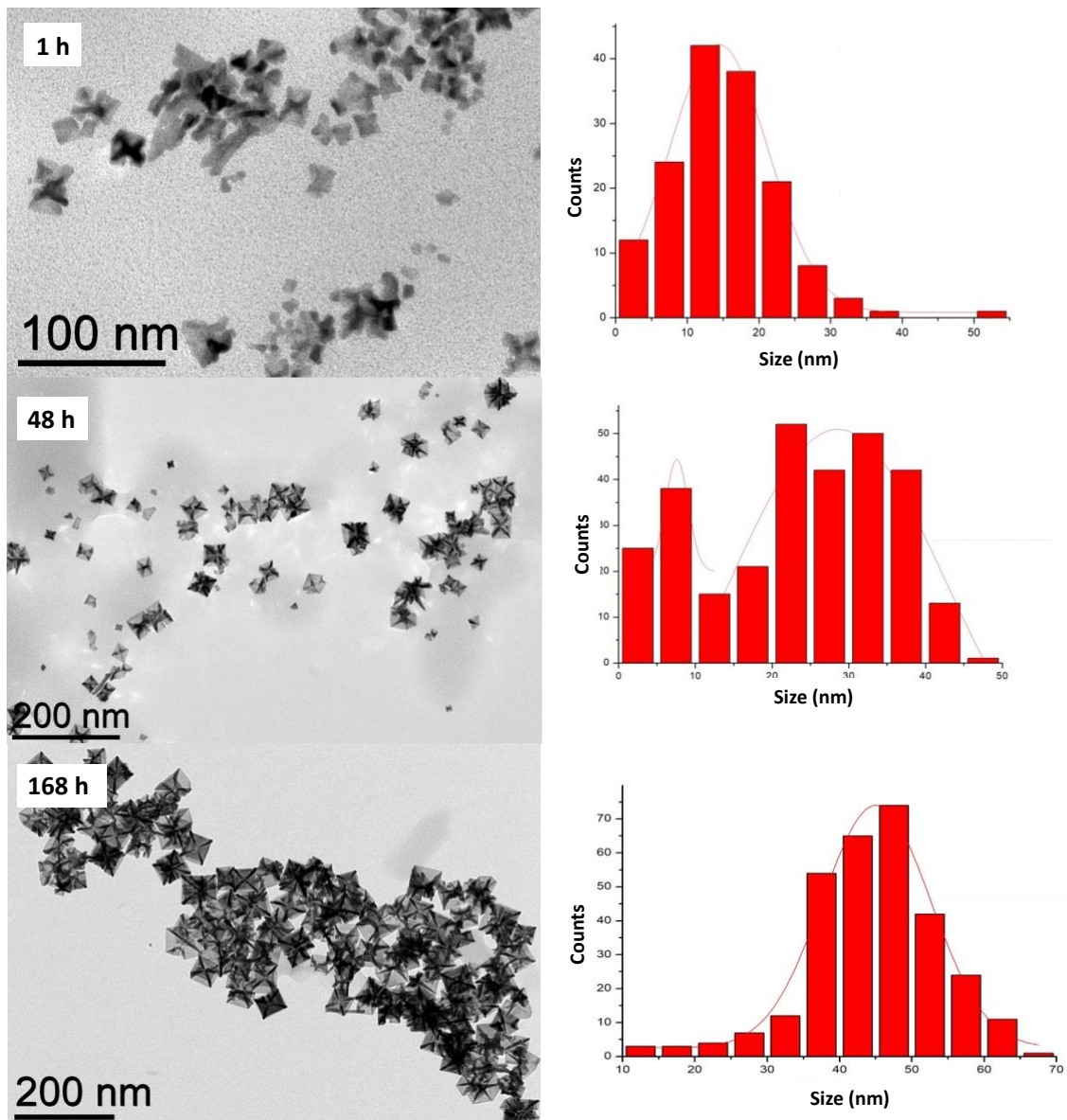


Fig. S3. Evolution in time of the concave nanocubes 1 h :  $14.4 \pm 6.9$  nm, 48 h: bimodal distribution  $7.5 \pm 1.5$  nm and 168 h:  $45.1 \pm 7.7$  nm.

## Shape evolution with temperature of the Pt nanoparticles

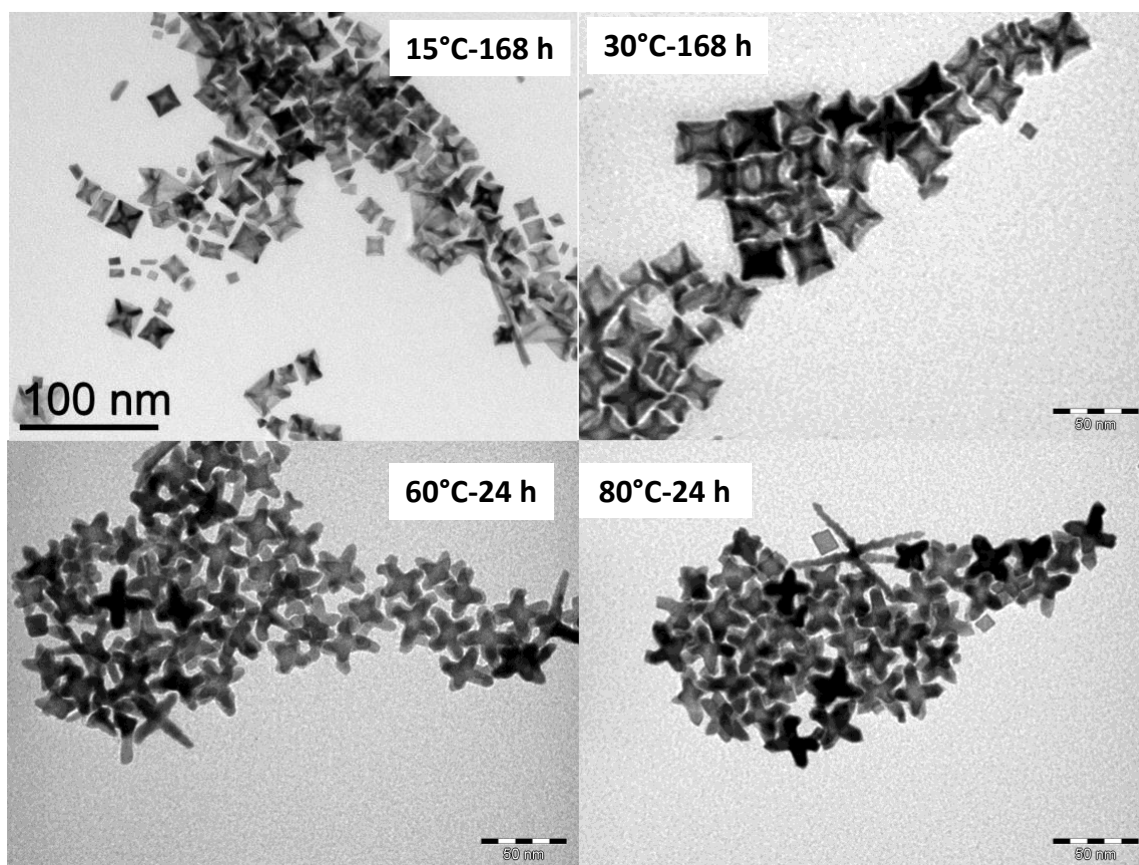


Fig. S4. Evolution of the nanoparticles shape with temperature. For the the 30°C, 60°C and 80°C scale bars are of 50 nm).

## XRD of the nano-objects obtained at 100°C

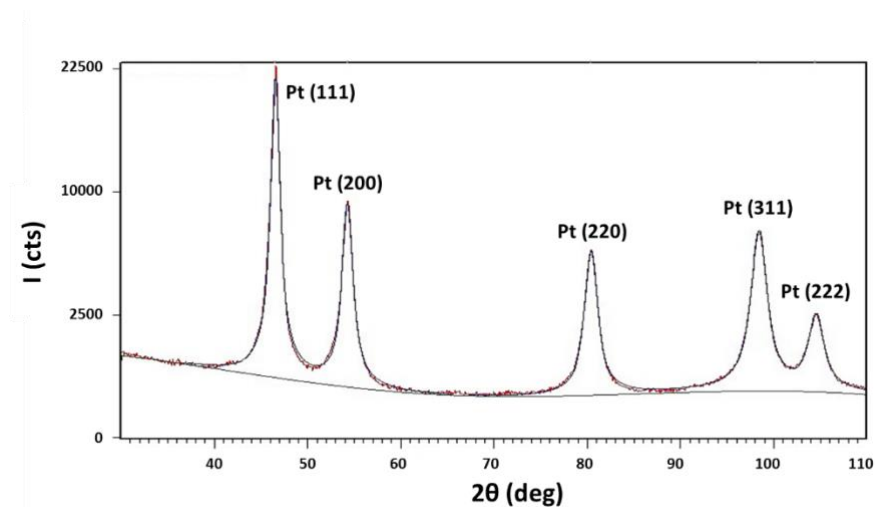


Fig. S5. XRD diffractogram of the nano-objects obtained at 100°C (Indexation of the peaks according to ICDD : 00-004-0802).

HRTEM of a long multipod arm and schematic representation of its 3D structure.

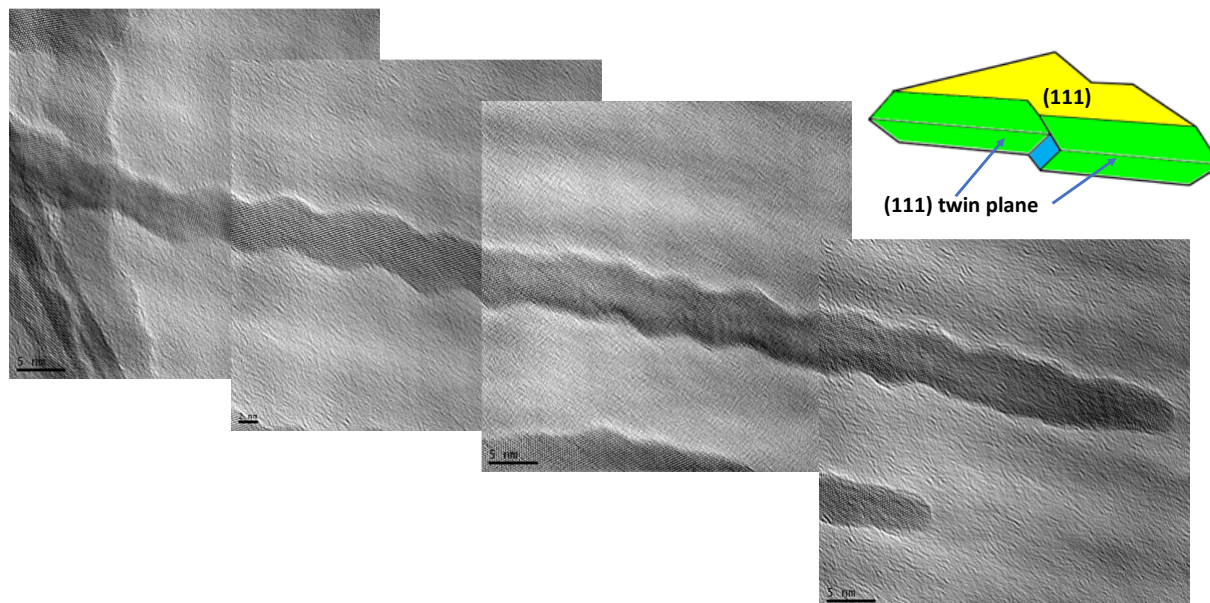


Fig. S6. HRTEM image of a whole multipod branch observed in Fig 2c and schematic representation of the 3D aspect of the arm. We propose the same structure as the one proposed in S. Maksimuk, X. Teng and H. Yang, J. Phys. Chem. C, 2007, **111**, 14312-14319.

Evolution in time of the reaction at 100°C

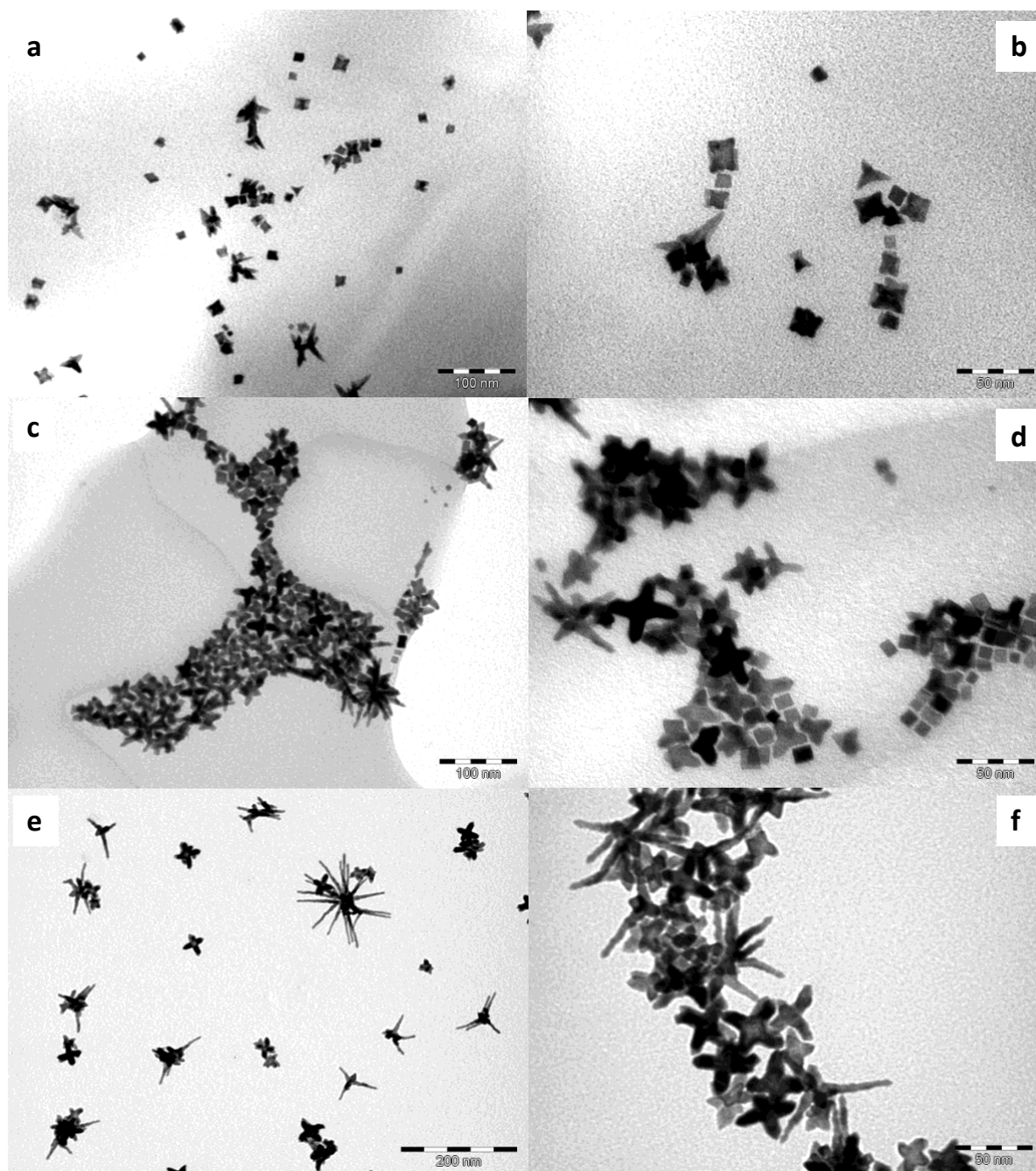


Fig. S7. Evolution of the nanoparticles shape with time at 100°C; a, b : 5 min , c, d: 20 min, e, f: 1 hour.

Scale bars: a, c: 100 nm; e: 200 nm; b, d, f: 50 nm.

TEM of the supernatant of the reaction at 25°C in the presence of Pt(111) support

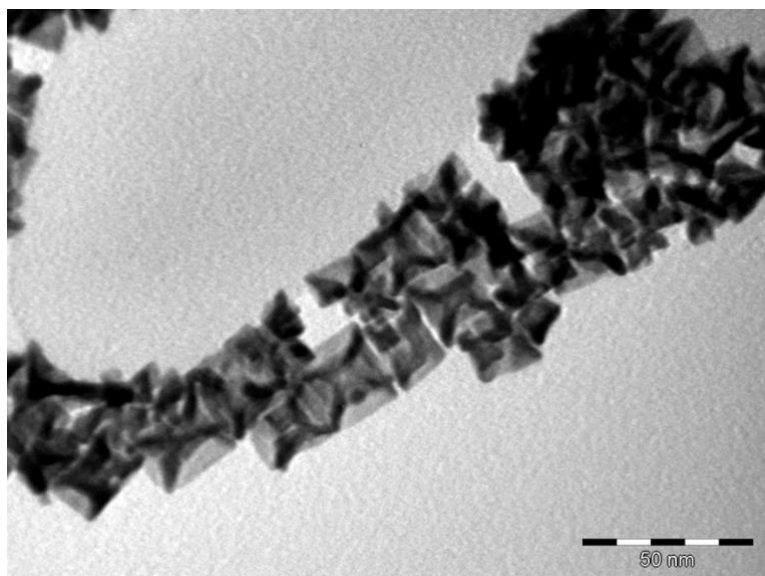


Fig. S8. TEM image of the supernatant of the reaction at 25°C showing the presence of concave nanocubes formed by homogeneous nucleation.

XRD measurement of the nano-objects growth over Pt(111) thin film :

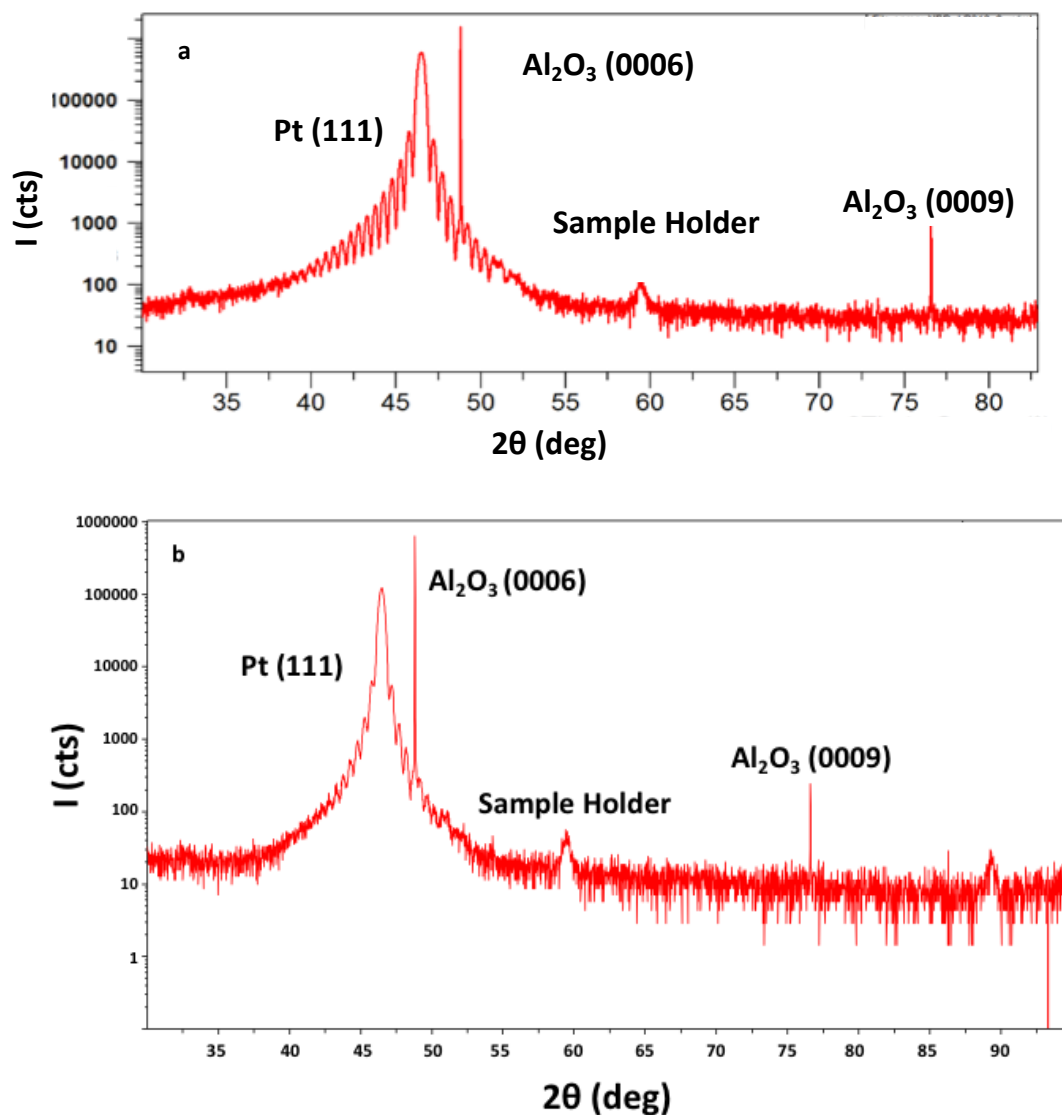


Fig. S9. X-Ray diffractograms confirming the orientation of the Pt nanostructures on the Pt(111) surface, since only the Pt(111) peak is present. (a) 25°C, (b) 100°C. The diffractograms present the (0001) orientation of the  $\text{Al}_2\text{O}_3$  substrate and the (111) orientation of Pt epitaxial film (with Pendellösung fringes). If Pt nanostructures were grown with a different growth orientation than (111), the peaks of the corresponding planes would be present (considering extinction conditions).

TEM of the supernatant of the reaction at 100°C in the presence of Pt(111) support

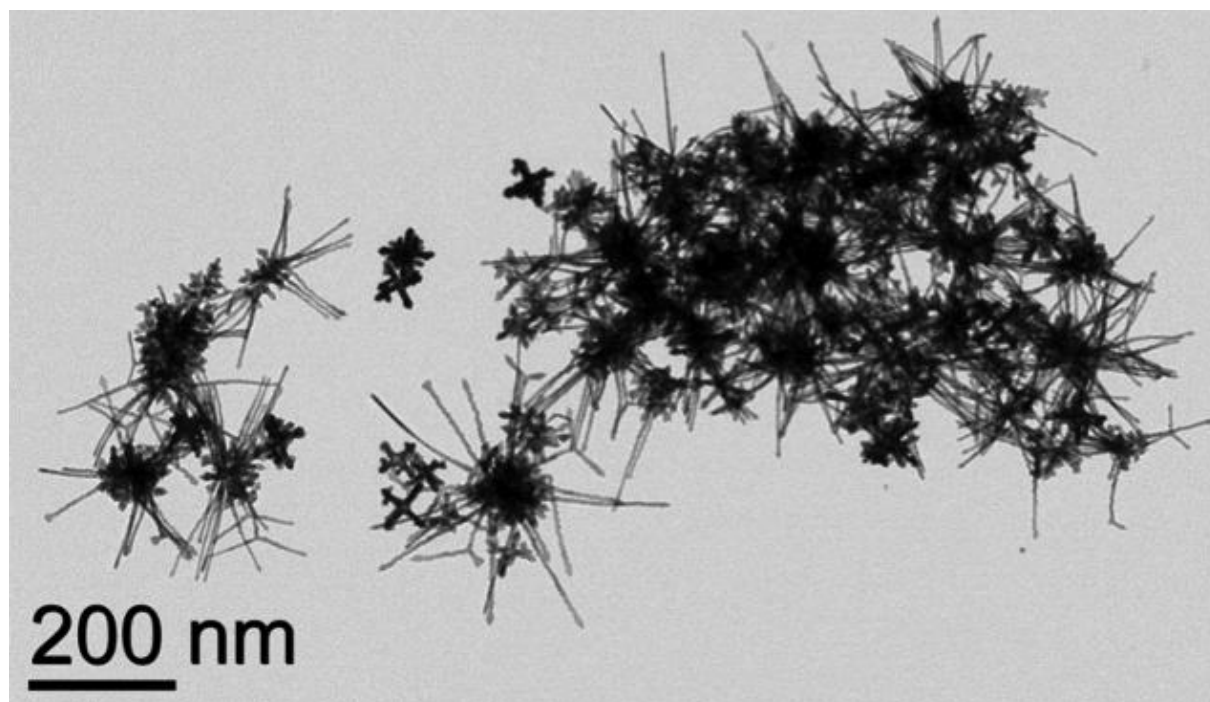


Fig. S10. TEM image of the supernatant of the reaction at 100°C showing the presence of dendritic octopods and multipods formed by homogeneous nucleation.